



Hand Radiographs in Skeletal Dysplasia: A Pictorial Review

Dheeksha D. S.¹ Stuti Chandola¹ Aayush Jain¹ Neerja Gupta² Madhulika Kabra² Manisha Jana¹

¹Department of Radiodiagnosis and Interventional Radiology, All India Institute of Medical Sciences, New Delhi, India

²Genetics Subdivision, Department of Pediatrics, All India Institute of Medical Sciences, New Delhi, India

Address for correspondence Manisha Jana, MD, DNB, FRCR, Department of Radiodiagnosis and Interventional Radiology, All India Institute of Medical Sciences, New Delhi 110029, India (e-mail: manishajana@gmail.com).

Indian J Radiol Imaging 2024;34:291–308.

Abstract

Skeletal dysplasias or osteochondrodysplasias comprise a large heterogeneous group of genetic disorders and possess significant overlap on imaging, which adds to the dilemma of the reporting radiologist. These entities are routinely evaluated with a detailed skeletal survey and hand radiographs form a crucial part of a complete survey. Certain conditions have characteristic imaging findings that enable a diagnosis be made on hand radiograph alone. Additionally, hand radiographs may also demonstrate findings that may be suggestive of a particular diagnosis/differential diagnoses and would warrant further assessment for proving the same. We aim to demonstrate the use of hand radiographs in diagnosis of various such entities through this review. Although they cannot replace a complete skeletal survey in the diagnosis, hand radiographs performed for other indications might alert a radiologist to the diagnosis of an unsuspected skeletal dysplasia.

Keywords

- ▶ skeletal dysplasia
- ▶ hand radiographs
- ▶ progressive pseudorheumatoid arthropathy
- ▶ mucopolysaccharidosis

Introduction

Skeletal dysplasias or osteochondrodysplasias comprise a large heterogeneous group of genetic disorders affecting the development of bone and cartilage, with more than 450 recognized disorders.^{1,2} Although they are individually rare conditions, together, they account for an average incidence of 1 in 5000 births and a prevalence of approximately 2.3 to 7.6 per 10,000 births according to various studies.^{1–4} A majority of these dysplasias lead to significant morbidity in the affected children, while some of them are lethal in the perinatal period.⁵ The diagnosis of this complex group of disorders requires the consolidation of clinical, laboratory, and radiological data. However, most of these dysplasias are notorious for significant clinical as well as imaging overlap, posing a diagnostic dilemma to the radiologist. A skeletal survey is routinely performed in the evaluation of a suspected case of skeletal

dysplasia; hand radiographs form a part of the complete survey. Accurate diagnosis is imperative because in addition to treating the child; it is crucial to provide genetic counselling to predict the outcome of future pregnancies.^{5,6}

Frontal radiographs of the hand and wrist are acquired in posteroanterior projection with a film focal distance of 100 cm. While imaging the nondominant hand suffices in bone age assessment, radiographs of both hands should be acquired when suspecting a skeletal dysplasia. ▶**Fig. 1A** demonstrates an optimally acquired normal hand radiograph.

Normal Ossification in Hand

The hand comprises a total of 21 bones that include 8 carpal, 5 metacarpal, and 14 phalanges.⁷ Among these, the carpal bones ossify directly via fibrous membrane (membranous ossification)

article published online
December 15, 2023

DOI <https://doi.org/10.1055/s-0043-1777320>.
ISSN 0971-3026.

© 2023. Indian Radiological Association. All rights reserved.
This is an open access article published by Thieme under the terms of the Creative Commons Attribution-NonDerivative-NonCommercial-License, permitting copying and reproduction so long as the original work is given appropriate credit. Contents may not be used for commercial purposes, or adapted, remixed, transformed or built upon. (<https://creativecommons.org/licenses/by-nc-nd/4.0/>)
Thieme Medical and Scientific Publishers Pvt. Ltd., A-12, 2nd Floor, Sector 2, Noida-201301 UP, India

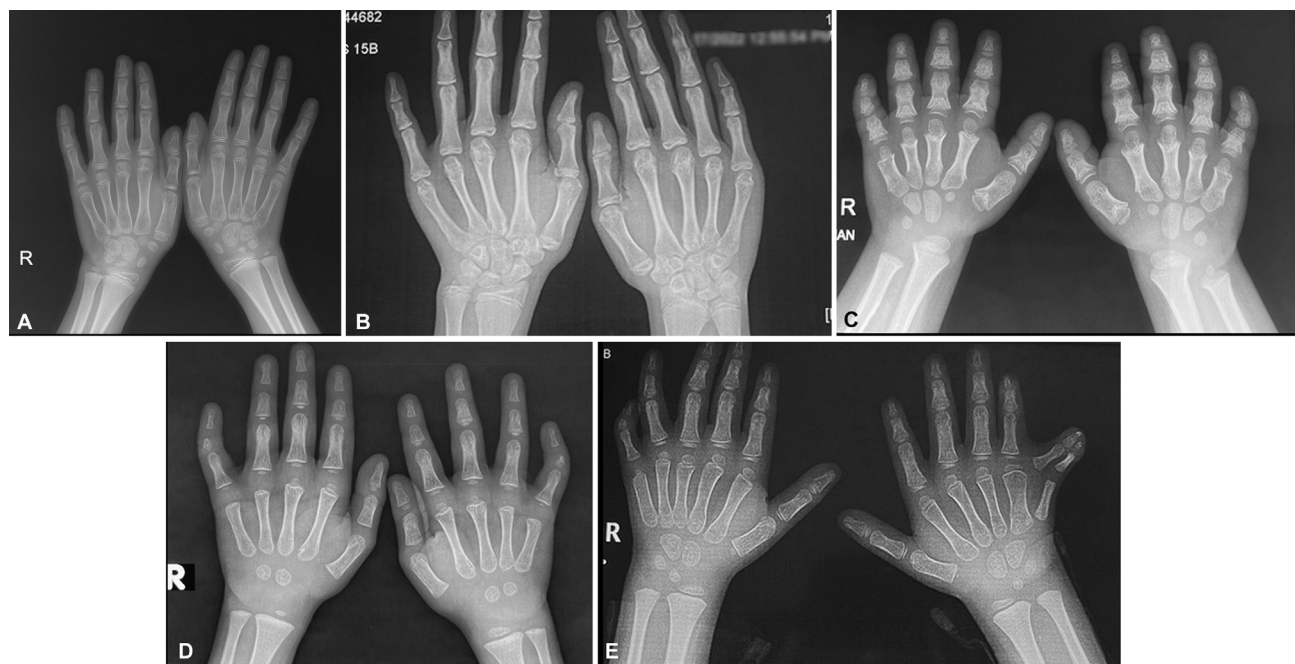


Fig. 1 Descriptive terms in the interpretation of hand radiographs: (A) Normal, (B) arachnodactyly, (C) short fingers in brachydactyly, (D) clinodactyly, and (E) synpolydactyly.

and eventually develop from a single ossification center, which is known as a primary ossification. The rest undergo endochondral ossification and develop secondary centers that appear in the cartilage of the extremities of the bone.^{7,8} The centrally ossified bone is the diaphysis, while the bone ossified from the secondary center is the epiphysis. Metaphysis is a part of the diaphysis that abuts on the epiphysis and represents the growing end of the bone.⁸ Initially the metaphysis and epiphyses are separated by a cartilaginous plate (known as physis or growth plate); ossification

of this plate results in union of the bone and eventual arrest of longitudinal bone growth.⁸ It is pertinent to note that the entire ossification process in general occurs earlier in females than males. Ossification and union age of the various bones of hand are shown in ►Table 1.⁸ Assessment of bone age is crucial in the diagnosis of skeletal dysplasias; however, it is beyond the scope of the article.

►Table 2 and ►Fig. 1 discuss the various descriptive terms used in the interpretation of hand radiographs.

Table 1 Appearance and fusion of ossification centers of various bones in hand and wrist^{7,8}

Bone	Appearance	Fusion
1. Carpal bones 1) Capitate and hamate 2) Triquetral 3) Lunate 4) Trapezium 5) Trapezoid 6) Scaphoid 7) Pisiform	2–4 months 2–3 years 3–4 years 3–4 years 4–6 years 4–6 years 9–12 years	–
2. Metacarpals	Diaphysis—present at birth Epiphyses: Females: 10 months–2 years Males: 14 months–3 years	Females: 13–15 years Males: 14–16 years
3. Phalanges	Appearance of centers occurs in characteristic ascending order: proximal phalanges, metacarpals, middle phalanges, and distal phalanges	Fusion of the epiphysis occurs in the following pattern: 1. Distal phalanges 2. Metacarpals 3. Proximal phalanges 4. Middle phalanges
4. Distal radius	~ 10–13 months	(fusion to shafts) Females: 15–17 years Males: 17–19 years
5. Distal ulna	~5–6 years	Females: 15–17 years Males: 17–19 years

Table 2 Descriptive terms and definitions

Term	Definition/description
Arachnodactyly	Long, spider leg-like fingers
Brachydactyly	Short fingers
Brachyphalangia	Shortened phalanges; Brachymesophalangia—shortened middle phalanges, brachytelephalangia—shortened distal phalanges
Camptodactyly	Flexed, bent fingers
Clinodactyly	Inward curvature of finger (usually of the fifth middle phalanx)
Ectrodactyly	Bifid/fork-like hand with fused fingers on either side of the hand
Polydactyly	Supernumerary fingers
Syndactyly	Fused fingers
Symphalangism	Fused phalanges

Conditions Where Hand Radiograph Is Diagnostic

Desbuquois Dysplasia

Desbuquois dysplasia is an autosomal recessive chondrodysplasia characterized by mutations in the CANT1 gene thereby leading to severe growth retardation, short extremities and multiple dislocations.⁹ Patients typically present within 6 years of age. Diagnostic findings on hand radiographs include short metacarpals (brachymetacarpism), bifid distal phalanx of the thumb, phalangeal dislocations, advanced carpal bone age, and delta phalanx, which refers to a longitudinally oriented bracketed small epiphysis located on the lateral aspect of the phalanx. It additionally lies parallel to the phalanx and thereby gives the appearance of a delta (►Fig. 2).¹⁰ Other supporting features include flattened proximal femoral metaphysis with a medial spike and exaggerated lesser tuberosity, thereby giving the “Swedish key” appearance, flattened acetabular roof, proximal fibular overgrowth, coronal spinal clefts, enlarged first metatarsals, and precocious tarsal bone age.^{9,10}

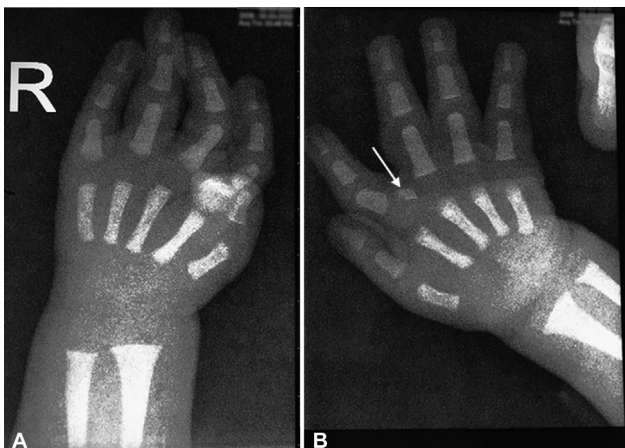


Fig. 2 Desbuquois dysplasia. Posteroanterior projectional radiographs (A and B) of bilateral hands demonstrate short metacarpals with a longitudinally oriented bracketed small “delta” epiphysis on the radial aspect of and paralleling the proximal phalanx of left middle finger (arrow).

Progressive Pseudorheumatoid Arthropathy

Progressive pseudorheumatoid arthropathy (PPRA), also known as progressive pseudorheumatoid dysplasia (PPRD), is a genetic skeletal dysplasia occurring due to a loss-of-function mutation in WNT-1 inducible signaling protein 3 (WISP3) gene that encodes for type II collagen, hence leading to progressive deterioration of articular cartilage.^{11,12} Usual presentation is between 3 and 6 years of age with painless stiffness and restricted movement in multiple joints, gait abnormalities, and bony enlargement of interphalangeal joints in hands.¹² Features of juvenile idiopathic arthritis (JIA), namely articular pain and morning stiffness, are typically absent in PPRD.^{11,12} Radiographic findings characteristic of this entity include metaphyseal expansion of proximal phalanges of hand and feet with associated flexion deformities or camptodactyly, which are usually most marked at proximal interphalangeal joints (►Fig. 3). Bone age is often delayed. Typical findings on lateral spine radiographs include gouge-shaped anterosuperior vertebral endplate defects with mild platyspondyly and kyphosis.^{11,12} Epiphyseal and metaphyseal enlargement with associated irregularity and flexion deformities in long bones are other supportive findings. Spine-related findings with preserved density and absence of periarticular bone erosions help to distinguish this entity from the more common JIA.¹²

Brachytelephalangi Chondrodysplasia Punctata

Chondrodysplasia punctata (CDP) refers to a heterogeneous group of epiphyseal dysplasias characterized by defective endochondral ossification and subsequent deposition of multiple calcific foci.^{13,14} Mutation in arylsulfatase gene has been identified in about 30% cases with plausible causal association with vitamin K deficiency.¹³ Patients with brachytelephalangi CDP present with facial dysmorphism in the form of mid facial hypoplasia, flat nose, hypertelorism along with short digits.^{13,14} Punctate calcifications and stippling in the vertebrae and in the epiphysis of the long bones are commonly observed, as in all CDPs.¹⁴ Imaging findings peculiar to this entity include calcific stippling in the craniocervical region, tarsal and carpal bones and vertebra with hypoplasia of phalanges, metacarpal and metatarsal bones,



Fig. 3 Progressive pseudorheumatoid arthropathy in a patient who initially presented with a clinical suspicion of juvenile idiopathic arthritis. Posteroanterior hand radiographs (A) demonstrate diffuse osteopenia and metaphyseal expansion involving the phalanges, which is the most marked at distal ends of the proximal phalanges (arrows). Periarticular erosions are distinctly absent. Lateral spine radiograph (B) shows mild platyspondyly (asterisks) with the characteristic “gouge-shaped” scooping erosions involving the anterosuperior ends of vertebral bodies (arrows, B).

and triangle-shaped hypoplastic distal phalanges being most characteristic (►Fig. 4).^{13,14} Craniocervical junction (CVJ) stenosis with subsequent spinal compromise is common; imaging of CVJ with computed tomography (CT) and magnetic resonance imaging (MRI) should, therefore, be offered in the neonatal period for early detection and stabilization.¹⁴

Angel Shaped Phalango-Epiphyseal Dysplasia

This rare genetic condition is characterized by disordered phalangeal development and ossification with an autosomal dominant pattern of inheritance.¹⁵ Age of presentation is variable; clinical features include extensive hyperextensibility of the fingers, swan neck deformity hypodontia, and precocious osteoarthritis of the hips.^{15,16} Hand radiographs demonstrate brachydactyly, delayed and incomplete ossifi-

cation of phalanges with pseudoepiphysis formation.¹⁶ These abnormalities are most pronounced in the middle phalanges, thereby resulting in the characteristic “angel shaped” phalanges, which is a result of defective epi-metadiaphyseal development. Resultant diaphyseal cuffing (representing the “wings” of an angel), surrounding the meta-diaphyseal region (body) with a cone-shaped epiphysis (“skirt”) and pseudoepiphysis (“head”) produces this appearance.¹⁵ (►Fig. 5) Carpal age is often delayed. Pelvic radiographs show delayed femoral head ossification, which evolve into small, fragmented epiphysis (similar to Perthes) with subsequent degeneration of the hip joint. Evaluation of other long bones shows a generalized delay of ossification of epiphyses and apophyses with Scheuermann like irregularities in spine.¹⁵

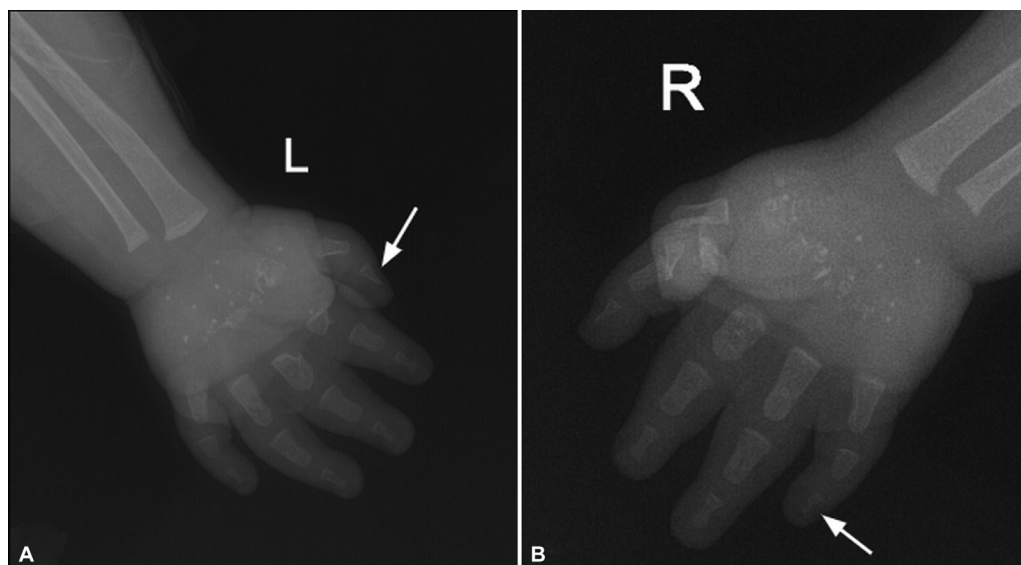


Fig. 4 Brachytelephalangi chondrodysplasia punctata in a 7 months' male infant patient. Posteroanterior hand radiographs (A and B) showing punctate stippling of carpal and metacarpal bones with hypoplastic phalanges, especially the distal phalanges that appear triangle-shaped (arrow).



Fig. 5 Angel shaped phalango-epiphyseal dysplasia. Hand radiograph (A) demonstrating brachytelephalangy (solid arrows). Magnified image (B) of the distal phalanges show variable morphology of the distal phalanges. The left fourth distal phalanx shows an “angel like” appearance. The arrowheads depict the hands, and the arrows, the skirt.

Albright's Hereditary Osteodystrophy

Pseudohypoparathyroidism type Ia (OMIM entry # 103580), also known as Albright's Hereditary Osteodystrophy (AHO), is an inherited metabolic disorder occurring due to maternal allelic loss of function mutation in the Gs-alpha isoform of the *GNAS* gene that ultimately leads to multihormonal end organ resistance.^{17,18} Common clinical features include short stature, obesity, round facies, and brachydactyly. Some patients have mental retardation with defective olfaction. Enamel hypoplasia and blunt root development are frequent dental defects.¹⁹ Laboratory findings include hypocalcemia and hyperphosphatemia, which resemble parathyroid hormone deficiency.¹⁹ Typical manifestations in hand radiographs include brachydactyly with brachymetacarpia and brachytelephalangy, which are most pronounced at III, IV, and V metacarpals and I distal phalanx and have been reported in approximately 70% of patients (→Fig. 6).¹⁸ Delayed bone age, osteopenia, and subcutaneous ossifications are other typical features.^{18,19}

Robinow Syndrome

Robinow syndrome is a heterogeneous disorder characterized by mesomelic or acromesomelic shortening of limbs, facial spinal, and genital anomalies.²⁰ Two major forms based on inheritance are recognized, namely the severe autosomal recessive and mild autosomal dominant varieties.

Clinically, there is short stature, midfacial hypoplasia with hypertelorism, short upturned nose with flat nasal bridge, tented upper lip and low set ears, and an occasional midline capillary hemangioma^{20,21}. Generally, the mesomelic shortening of the forearm is more striking than the shortening in the leg.

Radiographs demonstrate brachydactyly with shortening of the distal phalanx, fusion of the phalanges, and fusion of the carpal bones. A diagnostic feature is the splitting or clefting of one or more distal phalanges, especially that of the thumb (→Fig. 7).^{20,21} The radial head is dislocated (especially in recessive form) with Madelung deformity due to hypoplastic distal ulna.²¹ The latter finding is,



Fig. 6 Albright's hereditary osteodystrophy. Posteroanterior hand radiograph showing brachymetacarpia most marked at left third and bilateral fourth, and fifth metacarpals (arrows). Brachytelephalangy, especially in bilateral first and second digits, is also appreciated (arrowheads). The child had heterotopic nontraumatic ossifications over the face.

however, nonspecific and has other more common causes like exostosis and Leri-Weill dyschondrosteosis. Spinal radiographs show kyphoscoliosis with segmentation anomalies and hemivertebrae.²⁰ Genital abnormalities include micropenis, cryptorchidism, reduced clitoral size, and hypoplastic labia minora. The dominant variety presents with normal stature and mild mesomelic shortening with normal upper lip and few spinal abnormalities. Radial head dislocation is absent in this entity.^{20,21}

Hereditary Multiple Exostoses

Exostosis or osteochondromas are benign bone tumors of cartilaginous origin arising from the growth plate. Multiple

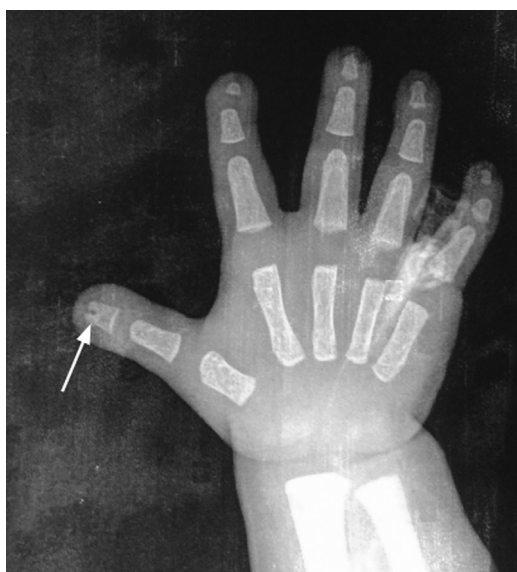


Fig. 7 Robinow syndrome. Radiograph of the left hand demonstrating brachydactyly with shortened distal phalanges and a longitudinal split in the distal phalanx of the thumb (arrow), which is a diagnostic for this entity.

exostoses occur as an autosomal dominant inherited condition, known as diaphyseal achalasia or hereditary multiple exostoses (HME).²² Positive *EXT* gene germline mutations on chromosomes 8, 11, and 19 have been linked to this condition.²³ Frequent sites of involvement include the distal femur, proximal tibia, wrist and hands, humerus, ankle, pelvis, and ribs. Osteochondromas in HME are more likely to be sessile than pedunculated.²² On radiographs, they are seen as bony outgrowths demonstrating medullary continuity with the parent bone and are directed away from the growth plate direction. The cartilaginous cap is difficult to identify on radiographs unless mineralized.^{22,23} These may cause a "bayonet hand" or pseudo-Madelung deformity in the upper limbs due to foreshortening of the ulna in relation to the radius, which has been reported in about one-third of patients (►Fig. 8)²³. Common complications include fractures, vascular compromise, impingement on nerves and tendons, overlying bursitis, and malignant transformation, which have been reported in up to 3 to 25% of patients.^{22,24} Suspicious features include growth after skeletal maturity, pain after physal closure, new onset cortical destruction, soft tissue, and a thickened cartilage cap more than 1.5 cm.^{22,23}

Ollier's Disease

Ollier's disease denotes the presence of multiple enchondromas, which are benign cartilaginous tumors. Coexistence of these tumors with osteochondromas is called metachondromatosis.^{24,25} Short bones of the hand are the most commonly predisposed site of involvement. Radiographs demonstrate multiple radiolucent lesions with narrow transition zone, sclerotic margins, and characteristic "rings and arcs, popcorn" varieties of chondroid calcification (►Fig. 9).²⁵ Rates of malignant degeneration to chondrosarcoma reach up to 50% in this condition, according to a recent study and MRI may be used as a screening method detecting malignant transformation in both HME and Ollier's disease.²⁴

Mucopolysaccharidosis

Mucopolysaccharidosis (MPS) is a group of disorders characterized by deficiency of enzymes responsible for the degradation of glycosaminoglycans (GAG). As a result, there is progressive multisystemic accumulation of GAGs. A gamut of skeletal abnormalities is seen in MPS, collectively termed as dysostosis multiplex. Hand radiographs in MPS show a claw hand deformity resulting from accumulation of GAGs in soft tissues. Short and thick metacarpals with proximal pointing are seen, with bullet-shaped phalanges. Carpal bones are hypoplastic, with dysplastic epi-metaphysis of the radius and ulna, resulting in a V-shaped deformity, which causes alteration in the carpal angle (►Fig. 10).²⁶

Mucopolipidosis

Mucopolipidosis (ML) is autosomal recessive lysosomal storage disorder that results in development of abnormal cell architecture and inclusion of intracytoplasmic bodies within the mesenchymal cells, particularly fibroblasts. Resultant overflow of lysosomal enzymes is seen into the serum/CSF/urine. Hand radiographs in ML demonstrate changes of dysostosis

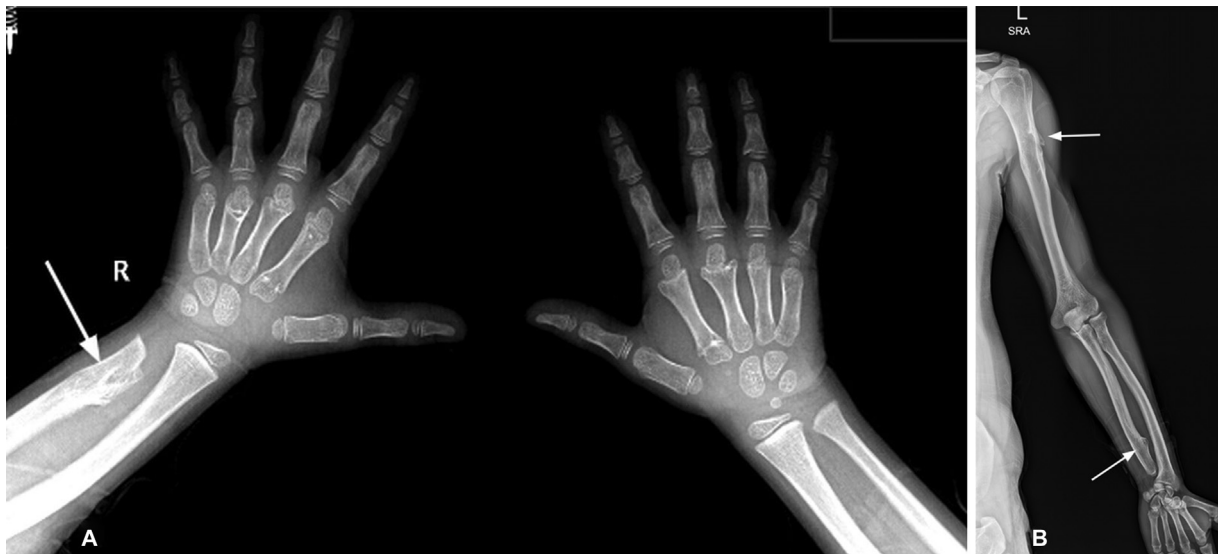


Fig. 8 Hereditary multiple exostosis. Posteroanterior hand radiographs (A) showing a sessile bony outgrowth in distal metaphysis of right ulna (arrow) suggestive of an osteochondroma. Mild bowing of the radius is also seen. Radiographs of left upper limb (B) showing multiple similar sessile and pedunculated outgrowths (arrows) in the long bones.

multiplex similar to MPS with proximal pointing of the metacarpals, diaphyseal thickening (undertubulation), and bullet shaped phalanges (► **Fig. 11**). Madelung deformity due to abnormal epi-metaphyseal development of the distal radius and ulna may also be seen. Since proximal pointing of metacarpals is also shared MPS, it is imperative to differ-

entiate between the two entities; periosteal thickening or cloaking at distal ulna and radius is an important feature observed in ML and is absent in MPS (► **Fig. 11**).²⁷

Diastrophic Dysplasia

Diastrophic dysplasia is a rare autosomal recessive skeletal dysplasia that manifests as shortened limbs, spinal abnormalities, joint abnormalities, and “Hitchhiker thumb.”²⁸ Clinically, patients have proximal abducted thumbs and great toe, joint contractures, short limbs, cleft palate, normal intellect, cervical kyphosis, and club feet. Radiographs demonstrate characteristic abducted, hypermobile, proximally placed thumb (hitchhiker’s thumb), marked shortening of the first metacarpal with irregular lengthened other metacarpals, ankylosis of proximal interphalangeal joints, and bizarre ossification of the hand bones (► **Fig. 12**).²⁸ Epiphyseal and metaphyseal irregularity in distal femur and tibia with V-shaped or chevron deformities are other features (► **Fig. 12**). The vertebral bodies also appear irregular.²⁸

Larsen Syndrome

Larsen syndrome is an autosomal dominant osteochondrodysplasia occurring due to mutation in the *FNLB* gene.²⁹ Clinical features include recurrent large joint dislocations, cylindrical fingers with broad fingertips (spatulate), and facial dysmorphism (midface hypoplasia, depressed nasal bridge and cleft palate). Radiological examinations show multiple joint dislocations along with vertebral anomalies. Hand radiographs demonstrate supernumerary carpal and tarsal bones, with small distal phalanges (particularly of the thumb) (► **Fig. 13**). Differentiation from desbuquois dysplasia is made on the basis of its autosomal recessive inheritance, presence of accessory ossification centers of metacarpals and phalanges, advanced carpal ossification, and hand deformities that are seen in DBDS.³⁰



Fig. 9 Ollier’s disease. Anteroposterior radiograph of the left forearm and wrist demonstrating few expansile lytic lesions with flocculent “popcorn” calcifications in the distal metadiaphyseal region of ulna (arrow) and fifth metacarpal suggestive of enchondromas. Associated bowing of the radius is also present.



Fig. 10 Mucopolysaccharidosis I. Radiograph of hand (A) demonstrating short and thick metacarpals, with proximal pointing (white arrow). Also note the bullet-shaped appearance of the phalanges (arrowheads) and dysplastic radial, ulnar epiphysis (asterisk). Lateral radiograph of the spine (B) showing anterior beaking (arrow) with a thoracolumbar kyphosis. Radiograph of the pelvis (C) showing rounded iliac blades (arrow), inferior tapering of iliac wings, and an underdeveloped acetabulum (asterisk, C). Lateral radiograph of the skull (D) showing a J-shaped sella (arrow).

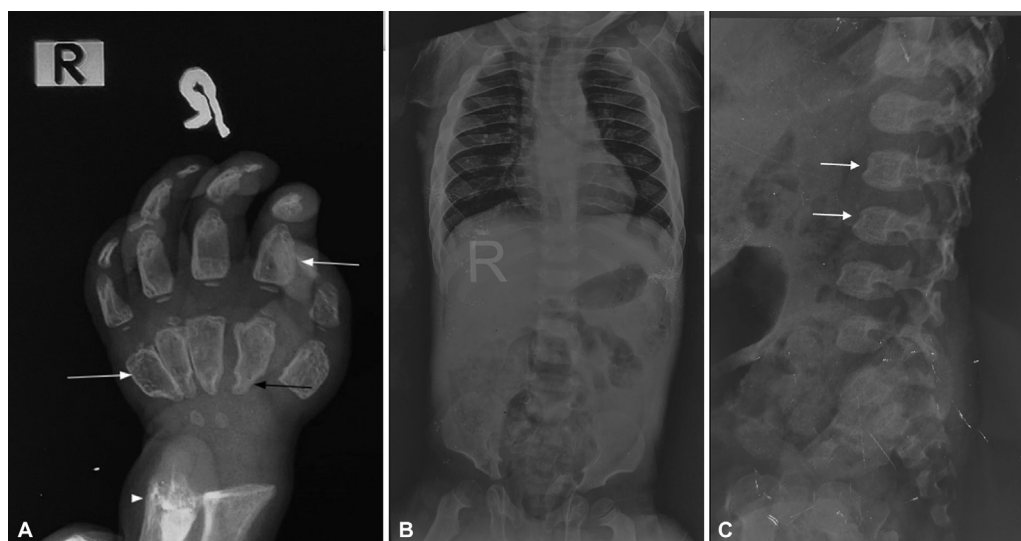


Fig. 11 Mucopolipidosis. Posteroanterior radiograph of the left hand (A) showing significant absence of the normal diaphyseal constriction (undertubulation—white arrows, A) in hand bones along with proximal pointing of the metacarpals (black arrow). The metaphysis of the radius and ulna is abnormal with shortening of the ulna and periosteal cloaking of ulna (arrowhead). Frontal and lateral radiographs of the spine (B and C) demonstrating anterior beaking within the vertebral bodies (arrows, b).

Rubenstein-Taybi Syndrome

Rubenstein-Taybi syndrome (also known as broad thumb syndrome) is a rare genetic disorder characterized by facial dysmorphism, intellectual disability and broad, angulated thumbs and great toes. Facial dysmorphism is in the form of an antimongoloid slant, beaked nose, and a high arched palate. Diagnosis is often evident clinically with an additive role of radiographs in supporting the diagnosis. Radiographs of the hand demonstrate a broad thumb which is angulated radially, with a delta (triangular) appearance of the 1st proximal phalanx.³¹ In addition, terminal broadening of the distal phalanges has been reported, along with clinodactyly of the fifth digit.³²

Conditions Where Hand Radiograph Are Suggested

These conditions have been summarized in ►Table 3.

Achondroplasia

Achondroplasia is the most common nonlethal skeletal dysplasia, resulting from a mutation in the gene affecting fibroblast growth factor receptor 3 and presenting with rhizomelic dwarfism. The abnormalities on hand radiographs include short and thick tubular bones, with widening of the space between the 2nd and 3rd digits, resulting in a trident hand deformity. Decreased distance between the epiphysis and metaphysis of the bone is seen, with the limbs of the metaphysis encompassing the epiphysis resulting in a “V”/chevron deformity and apparent widening of the joint spaces (►Fig. 14).^{33,34}

Osteogenesis Imperfecta

Osteogenesis imperfecta (OI), also known as “brittle bone disease,” is an osteopenic skeletal dysplasia occurring due to mutations in the genes responsible for polypeptide arrangement in collagen, resulting in altered biomechanical



Fig. 12 Diastrophic dysplasia. Clinical images (A and B) showing limb shortening with abducted thumb (A) and great toes (B) representing the characteristic Hitchhiker deformity. Hand radiograph (C) demonstrating markedly shortened first metacarpal bilaterally (arrows, C). Other metacarpals appear shortened and irregular (asterisks) with bizzarrelly ossified carpal bones (short arrows). The distal radial epiphyses are widened, irregular, and "V" shaped. Knee radiograph (D) showing epimetaphyseal enlargement and irregularity in distal femur and proximal tibia that appear chevron shaped (arrows, D).

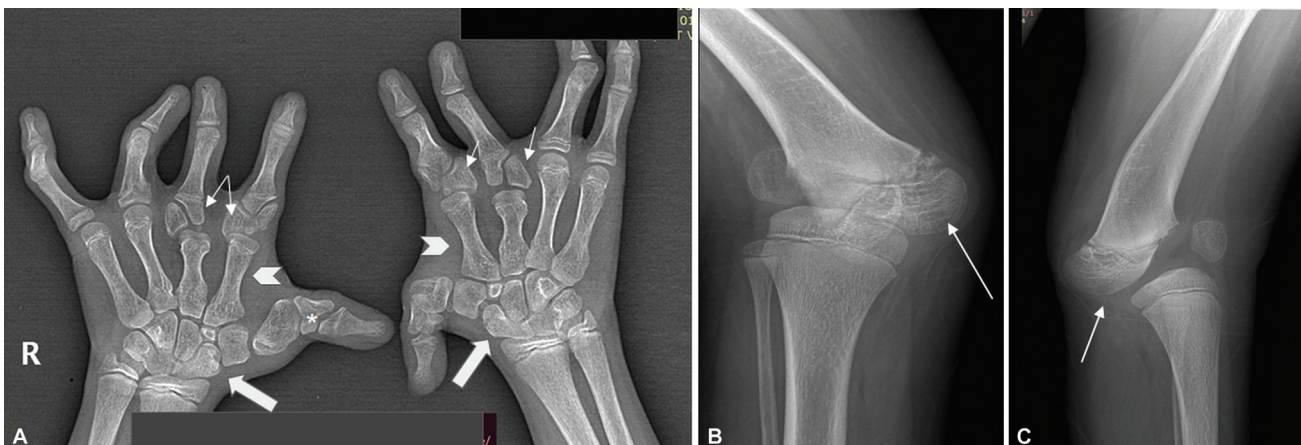


Fig. 13 Larsen syndrome. Hand radiograph (A) showing supernumerary carpal bones (solid arrows) with shortening of the metacarpals (arrowheads). Also note significant shortening of the phalanges of the thumb (asterisk) and accessory ossification centers for the proximal phalanges (arrows). Frontal and lateral radiographs of the left knee (B and C) showing dislocation of the knee joint with medial and anterior displacement of the femoral condyle over the tibia (arrows).

properties in the involved tissues. This is responsible for the radiographic features, which include osteopenia, multiple fractures, and progressive skeletal deformities. Several types of OI have been described, with varying severity and radiographic findings. Hand radiographs in OI show significant osteopenia with cortical thinning, along with thinned out

metacarpals (→Fig. 15).³⁵ Deformities secondary to prior fractures may also be seen.³⁶

Osteopetrosis

Osteopetrosis (also known as marble bone disease) is a sclerosing bone dysplasia, characterized by a failure of

Table 3 Conditions where the hand radiograph is suggestive of an underlying skeletal dysplasia

Condition	Findings on hand X-ray	Other findings on skeletal survey
Achondroplasia	Trident hand	Trident pelvis, progressive narrowing of lumbar interpedicular distance, rhizomelic long bone shortening, “tombstone” pelvis
Osteogenesis imperfecta	Thin osteopenic metacarpals and phalanges	Multiple vertebral platyspondyly, thin long bones with bowing and fractures/ deformity, multiple Wormian bones
Osteopetrosis	Sclerotic bones with “bone within bone” appearance	Generalized osteosclerosis, “sandwich” vertebrae, similar long bone appearance
Pyknodysostosis	Sclerotic bones, acro-osteolysis of distal phalanges	Obtuse mandibular angle, multiple Wormian bones, open sutures, “spool shaped” vertebral bodies
Hajdu-Cheney syndrome	Band acro-osteolysis of distal phalanx	Bulging of the squamous occipital bone, Wormian bones, platybasia, aplasia of the frontal sinuses
Metaphyseal chondrodysplasia	Irregularity and sclerosis of metaphyses of wrist joint and short long bones of the hand	Similar appearance of other metaphyses
Spondylometaphyseal dysplasia	Irregularity and sclerosis of metaphyses of wrist joint Metaphyseal “corner fracture” in a variant	Similar appearance of other metaphyses Variable vertebral changes
Ellis-van Creveld syndrome	Postaxial polydactyly, carpal coalition (capitate and hamate), and fusion of the metacarpals	Outward curve of humeri, delayed ossification of the lateral tibial condyle and proximal tibial exostosis, trident pelvis
Acromicric dysplasia	Delayed bone age with shortening of the metacarpals and phalanges, internal notching of the second and external notching of the fifth metacarpals	Similar changes in the feet
Acromesomelic dysplasia	Short and broad hand bones with cone shaped epiphysis	Supra-acetabular notch, shortening of the dorsal margins of the vertebrae with a ventral protrusion
Multiple epiphyseal dysplasia	Small irregular sclerotic carpal bones and epiphyses	Similar epiphyseal changes around other joints of the body, double-layered patella (in autosomal recessive variant)
Thanatophoric (► Fig. 23)	Trident hand	Trident pelvis, platyspondyly, “telephone handle” femora
Pseudoachondroplasia (► Fig. 24)	Delayed bone age, small irregular epiphyses, wide flared metaphyses, cone shaped metaphyses, small metacarpals	Central “tongue-like” protrusion of anterior vertebral bodies Delayed ossification of femoral head and y cartilage
Cleidocranial dysostosis (► Fig. 25)	Accessory epiphysis at the base of second metacarpal	Pseudo pubic diastasis Absent/hypoplastic clavicles

osteoclast development or maturation, resulting in impaired resorption of the primary spongiosa and hence dense bones (however more prone to fractures due to reduced bone mass). Multiple subtypes have been described, based on the age of presentation and severity. The autosomal recessive form has been described with multiple fractures in utero and generalized osteosclerosis with narrowing of the skull base foramina. The autosomal dominant form presents in childhood and adolescents with increased bone density, characteristic “sandwich vertebrae,” and narrowing of the normal medullary cavity of long bones.³⁷ Hand radiographs demon-

strate generalized osteosclerosis with obliteration of the medullary cavity. In addition, the primitive (endobones) may be seen replacing the medullary cavity, resulting in a “bone within bone” appearance (► Fig. 16). The distal radius and ulna may show alternating dense transverse bands.³⁸

Pyknodysostosis

Also known as Maroteaux-Lamy dysplasia, pyknodysostosis is another sclerosing bone dysplasia that results from impaired osteoclast function. Clinical presentation is in the form of short stature and hypoplasia of the midface. Hand

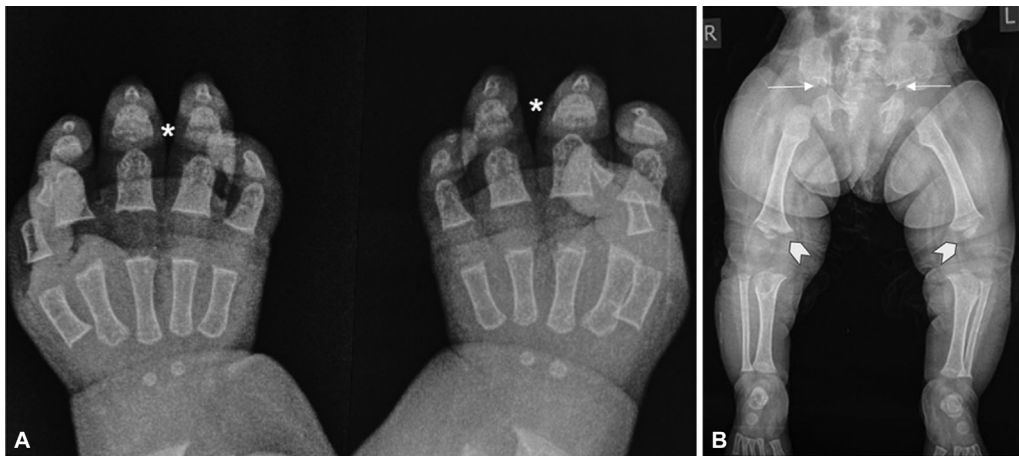


Fig. 14 Achondroplasia. Hand radiographs (A) demonstrating short and tubular hand bones with widened space between the second and third digits (asterisks), known as the trident hand deformity. Radiograph of the pelvis and bilateral lower limbs (B) showing squared iliac blades with trident acetabuli (black arrows) along with rhizomelic shortening of bilateral femori. The distal femoral epiphyses are small with the flared metaphyses forming a “V” or a chevron deformity (arrowheads) at bilateral knee joints.

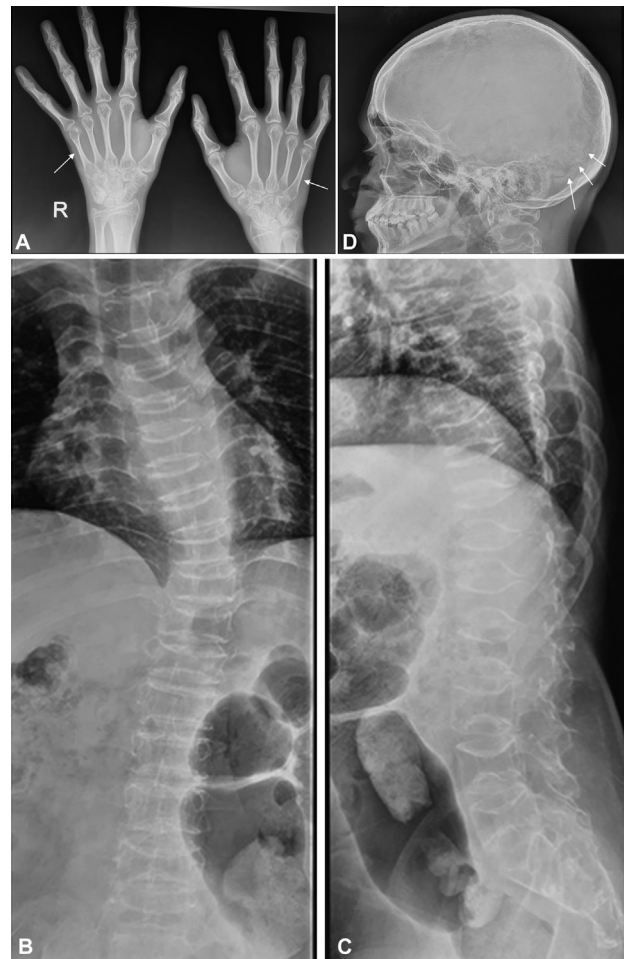


Fig. 15 Osteogenesis imperfecta. Hand radiograph (A) showing osteopenia with slender and thinned out metacarpals with associated cortical thinning (white arrows). Radiographs of the dorsolumbar spine (B and C) showing significant osteopenia with biconcave collapse of the vertebral bodies and resultant scoliotic deformity. Lateral radiograph of the skull (D) showing multiple Wormian bones (arrows).

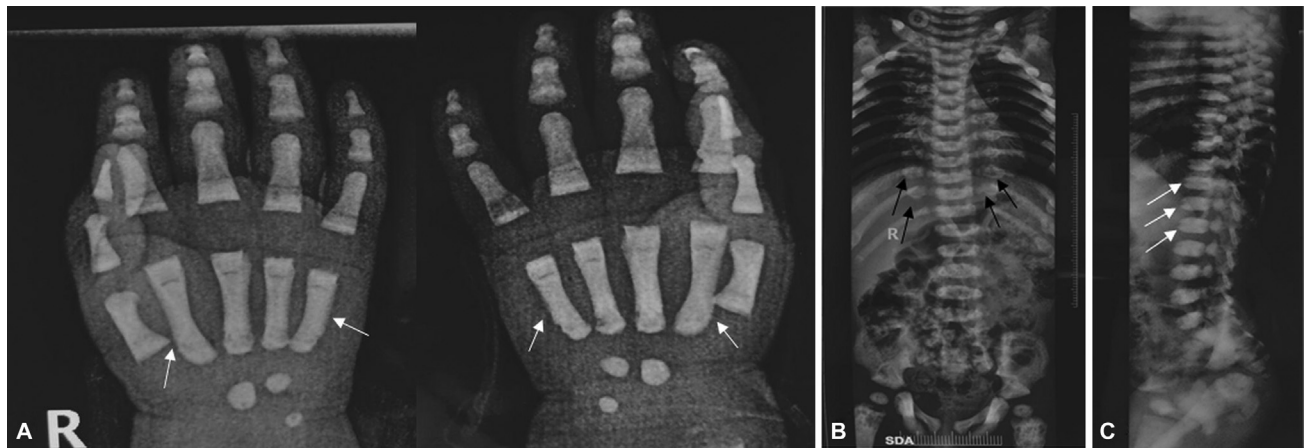


Fig. 16 Osteopetrosis. Hand radiographs (A) showing loss of the medullary cavity within the bones with well-defined “endobones” replacing the same (arrows). Radiographs of the dorsolumbar spine (B) and (C) showing generalized increased bone density with maintained vertebral height (white arrows, C). There is mild bulbous prominence of the posterior ends of the ribs suggestive of extramedullary hematopoiesis (black arrows, B).

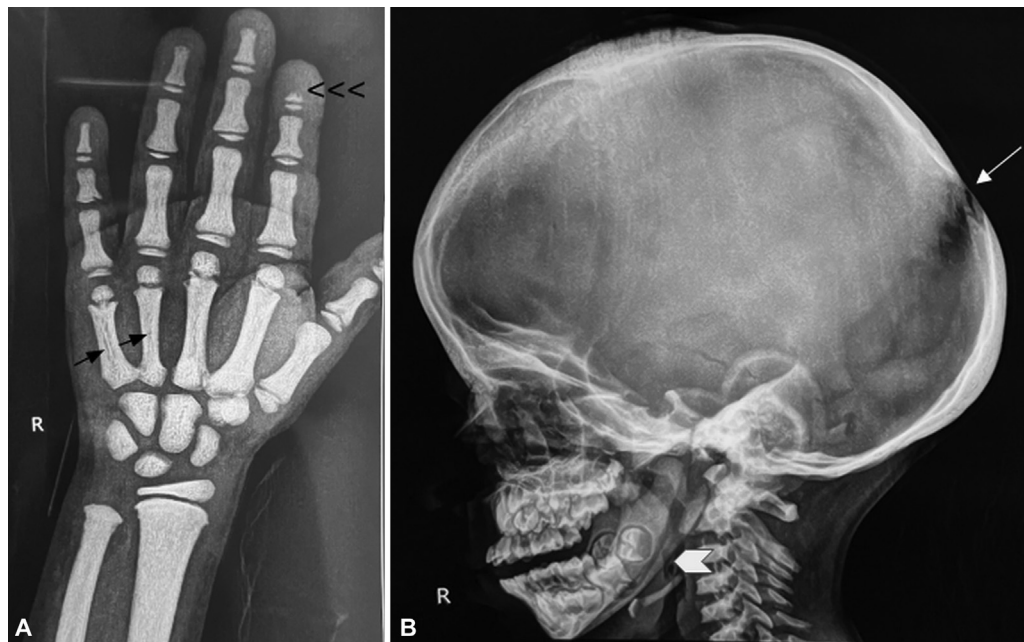


Fig. 17 Pyknodysostosis. Radiograph of the right hand in a 7-year-old girl (A) showing generalized increase in bone density with preservation of the medullary cavity (arrows). Resorption of the tuft of the second terminal phalanx is seen (arrowheads), suggestive of acro-osteolysis. Lateral radiograph of the skull (B) showing an obtuse mandibular angle (arrowhead) along with an open posterior fontanelle (arrow).

radiographs demonstrate generalized increase in bone density with a preserved medullary cavity. In addition, there is resorption of the terminal phalangeal tips (acro-osteolysis) (–Fig. 17).³⁸ Preservation of the medullary cavity, presence of acro-osteolysis, and widely open anterior fontanelle along with an obtuse mandibular angle help to differentiate pyknodysostosis from osteopetrosis on radiographs.

Hajdu-Cheney Syndrome

Hajdu-Cheney syndrome is a rare autosomal dominant disorder of the connective tissue that occurs as a result of

mutation in the NOTCH2 gene responsible for regulation of skeletal development and bone remodeling. Hajdu-Cheney syndrome presents clinically with short stature, progressive shortening of fingers and toes, and a flat facial profile with coarse hair. Predominant radiological findings include abnormalities of the cranial vault (bulging of the squamous occipital bone, Wormian bones, platybasia, aplasia of the frontal sinuses) along with band acro-osteolysis in the hands and feet.³⁹ Band acro-osteolysis appears as a linear band of lucency just distal to the proximal end of the terminal phalanx, and is characteristic of this condition.⁴⁰

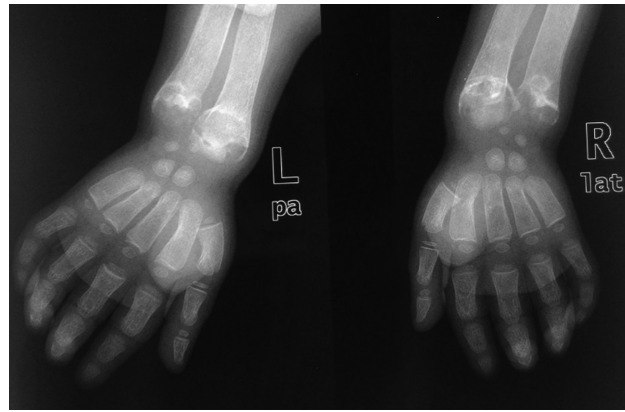


Fig. 18 Metaphyseal chondrodysplasia (Jansen type). Hand radiograph showing significant metaphyseal irregularity with associated sclerosis involving the distal metaphysis of the bilateral radii and ulna. Metaphyses of the rest of hand bones are normal.

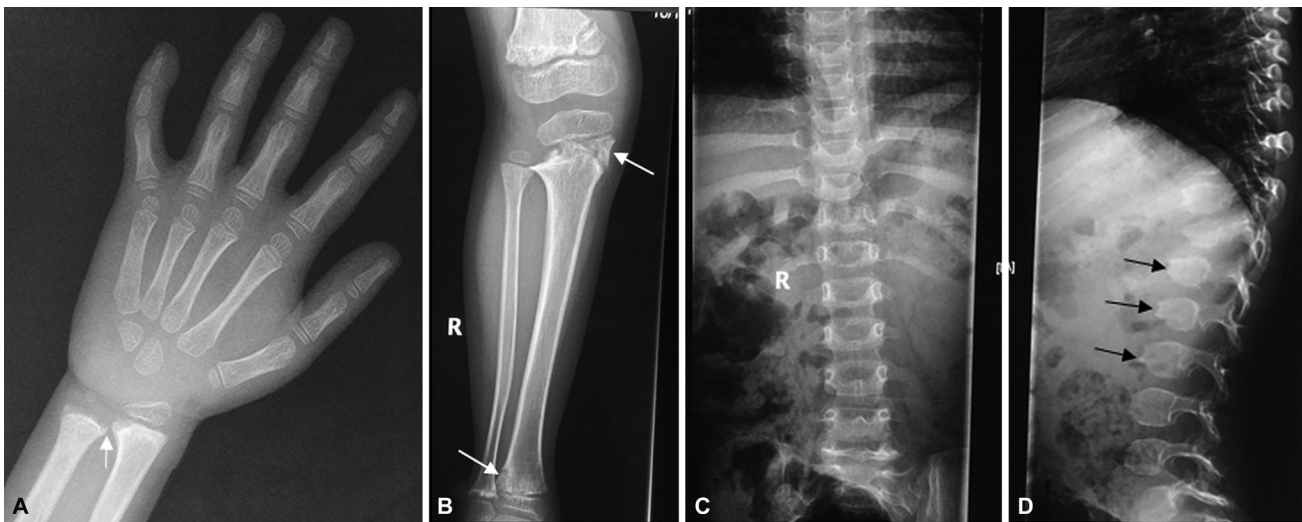


Fig. 19 Spondylometaphyseal dysplasia (Sutcliffe type). Frontal radiograph of the left hand (A) showing metaphyseal corner fractures involving the distal ulna (arrow). Frontal radiograph of the right leg (B) showing metaphyseal corner fractures involving the medial end of the right proximal and lateral end of the right distal tibia (white arrows). Radiographs of the dorsal spine (C and D) showing ovoid shape of the vertebral bodies (black arrows).

Metaphyseal Chondrodysplasia

Metaphyseal chondrodysplasia (MCD) is a group of disorders, with dysplastic development of the metaphysis of long bones. Depending on the predominant various types of bone involvement, they are classified into different subtypes. Of them, Jansen type MCD is the one that commonly affects the short long bones of the hand and the wrist joint (► Fig. 18).⁴¹

Spondylometaphyseal Dysplasias

Spondylometaphyseal dysplasias are a group of disorders wherein the spine is also affected in addition to the long bone metaphysis. Various subtypes are described. Of them, Sutcliffe type/corner fracture type presents with metaphyseal corner fractures around the wrist joints (► Fig. 19). When suspected on hand radiograph; a spine radiographic finding of ovoid vertebrae; and corner fractures around hip and knee joints confirm the radiological diagnosis (► Fig. 19).⁴²

Ellis-van Creveld Syndrome

Ellis-van Creveld syndrome (also known as chondroectodermal dysplasia) is a cause of mesomelic shortening of bones, characterized by cardiac anomalies, genu valgum, and dysplastic nails and teeth. Radiological findings include shortening of the forearm and leg bones, delayed ossification of the lateral tibial condyle, and proximal tibial exostosis along with a trident shaped acetabulum. Hand radiographs demonstrate postaxial polydactyly, carpal coalition (capitate and hamate), and fusion of the metacarpals (► Fig. 20).⁴³

Acromicric/Acromesomelic Dysplasia

Acromicric dysplasia is a rare bone dysplasia that presents with short stature, short hands and feet, and facial dysmorphism (round facies, bulbous nose, prominent philtrum). Classical radiographic abnormalities in the hand include delayed bone age with shortening of the metacarpals and phalanges, internal notching of the second metacarpals, and



Fig. 20 Ellis-van Creveld syndrome. Radiograph of both hands (A and B) showing bilateral postaxial polydactyly with fusion of the metacarpals for the third, fourth and fifth, sixth digits bilaterally (arrows, A and B). Radiograph of the chest (C) showing a narrow thoracic cage with outwardly curved bilateral humeri (arrows). Bilateral lower limb radiograph (D) showing shortening of the leg bones, suggestive of mesomelic shortening with trident pelvis (arrows).

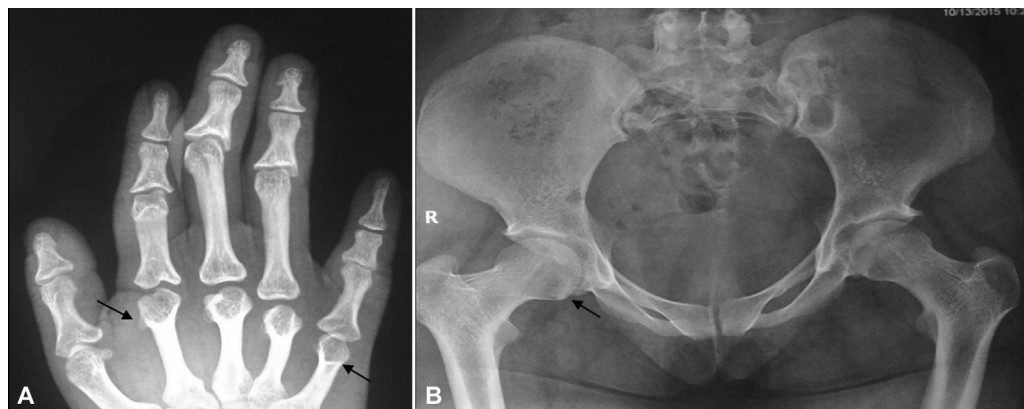


Fig. 21 Acromicric dysplasia. Hand radiograph (A) demonstrating brachymetacarpia (arrows) and brachydactyly with subluxation at third proximal interphalangeal joints and internal notching of the 2nd metacarpal. Radiographs of pelvis (B) showing internal notching of femoral head (arrow).

external notching of the fifth metacarpals. These notches tend to disappear in adulthood (→ Fig. 21).⁴⁴

Acromesomelic dysplasias are characterized by severe short stature with shortening of the middle and distal segments. Head is disproportionately large with flattening of the midface. Radiographs demonstrate short and broad hand bones with cone-shaped epiphyses and shortening of the forearm bones. Spine

radiographs show shortening of the dorsal margins of the vertebrae with a ventral protrusion.⁴⁵ A supra-acetabular notch on pelvis radiograph is also characteristic (→ Fig. 22).

Segment-Wise Approach

A concise segment-wise approach is summarized in → Table 4.

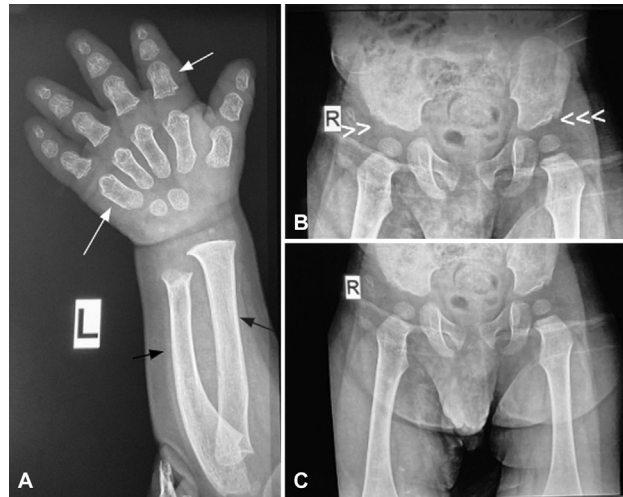


Fig. 22 Acromesomelic dysplasia. Radiograph of the left hand (A) showing short and broad hand bones (white arrows) along with shortening of the forearm bones (black arrows). Radiographs of pelvis and proximal femora (B and C) showing supra-acetabular notches (arrowheads), which are characteristic of this condition.

Table 4 Segment-wise imaging findings and their diagnostic implications

Segment	Finding(s)	Diagnostic implications
Distal radius and ulna	Madelung deformity	MPS, mucopolisidosis
	Metaphyseal flaring and irregularity, widened growth plate, osteopenia	Rickets
	Metaphyseal irregularity, sclerosis, no osteopenia	Metaphyseal chondrodysplasia, spondylometaphyseal dysplasia
	Pseudo-Madelung deformity, visible exostoses	Hereditary multiple exostoses
	Lytic lesions with chondroid matrix; may be multiple	Enchondromatosis
	Lytic lesions with ground glass matrix	Fibrous dysplasia (mono/polyostotic)
Carpal bones	Delayed bone age	Congenital hypothyroidism, rickets, spondyloepiphyseal dysplasia congenita, multiple epiphyseal dysplasia, pseudoachondroplasia, etc.
	Advanced bone age	Desbuquois dysplasia, Kniest syndrome
	Supernumerary carpal bones	Larsen syndrome
	Carpal coalition	Ellis-van Creveld
	Stippling	Chondrodysplasia punctata and its subtypes
Metacarpals	Short metacarpals (brachymetacarpia)	Acromesomelic and acromicric dysplasia, pseudoachondroplasia
	Short fourth metacarpal	Albright's hereditary osteodystrophy (pseudohypoparathyroidism)
	Thin long metacarpals	Marfan syndrome, osteogenesis imperfecta
Phalanges	Short distal phalanges	Brachytelephalangic chondrodysplasia punctata
	Acro-osteolysis	Pycnodysostosis, Hajdu-Cheney disease
	Metaphyseal expansion of proximal phalanges	Pseudorheumatoid arthropathy
	Longitudinal split of distal phalanges	Robinow syndrome
	Angel shaped phalanges	ASPED
	Delta phalanx	Desbuquois dysplasia

Abbreviations: ASPED, angel-shaped phalango-epiphyseal dysplasia; MPS, mucopolysaccharidosis.

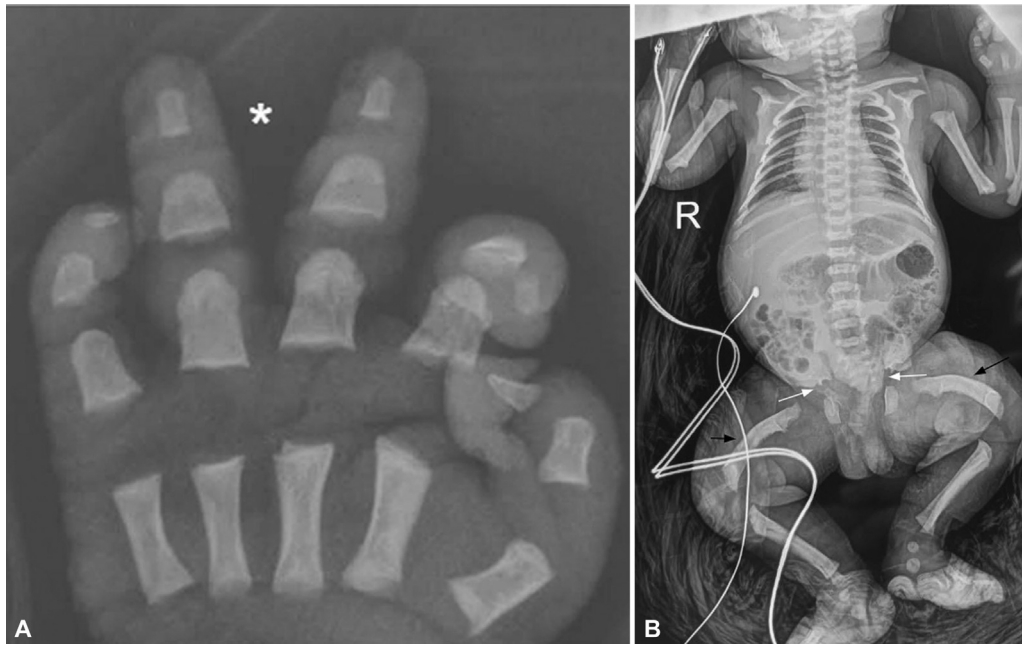


Fig. 23 Thanatophoric dysplasia. Hand radiograph (A) of a newborn with thanatophoric dysplasia showing short hand bones with a separation in between the middle and ring fingers (asterisk) suggestive of trident hand. Infantogram (B) demonstrating hypoplastic iliac blades with trident acetabuli (arrows), rhizomelic shortening in bilateral femoris that characteristically show telephone handle appearance (black arrows).

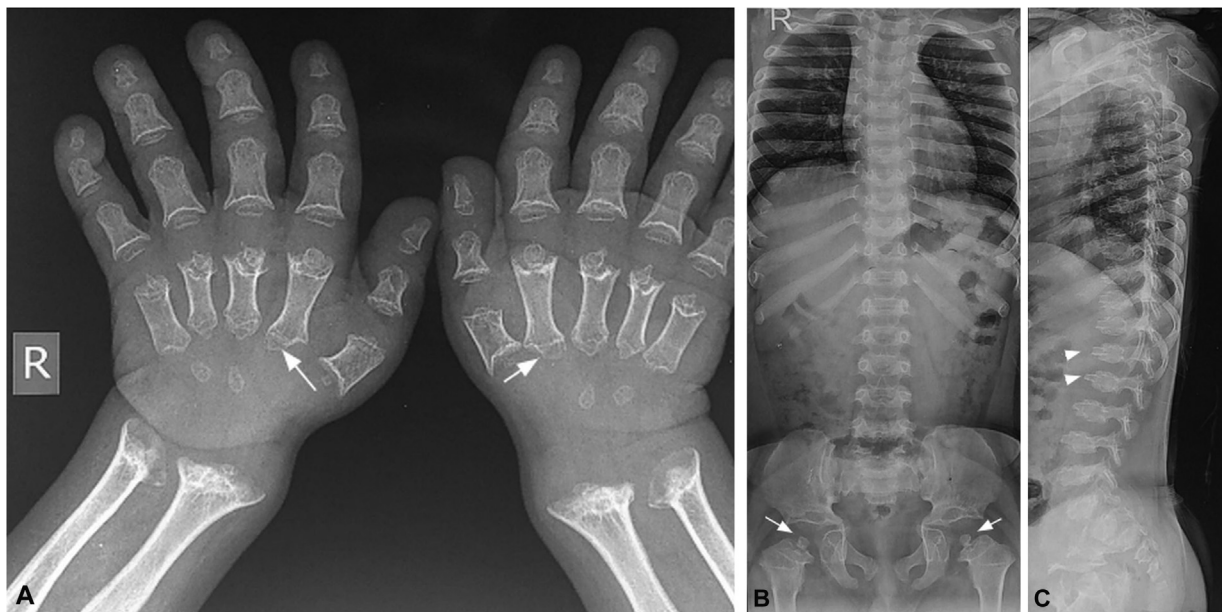


Fig. 24 Pseudoachondroplasia. Hand radiograph (A) showing small irregular epiphyses with flared metaphyses in the hand bones and small metacarpals (arrows, A), diffuse osteopenia, and markedly delayed bone age. Frontal (B) and lateral (C) projections of spine radiographs showing central “tongue-like” protrusion of anterior vertebral bodies (arrowheads, C) with small irregular femoral heads (arrows, B).

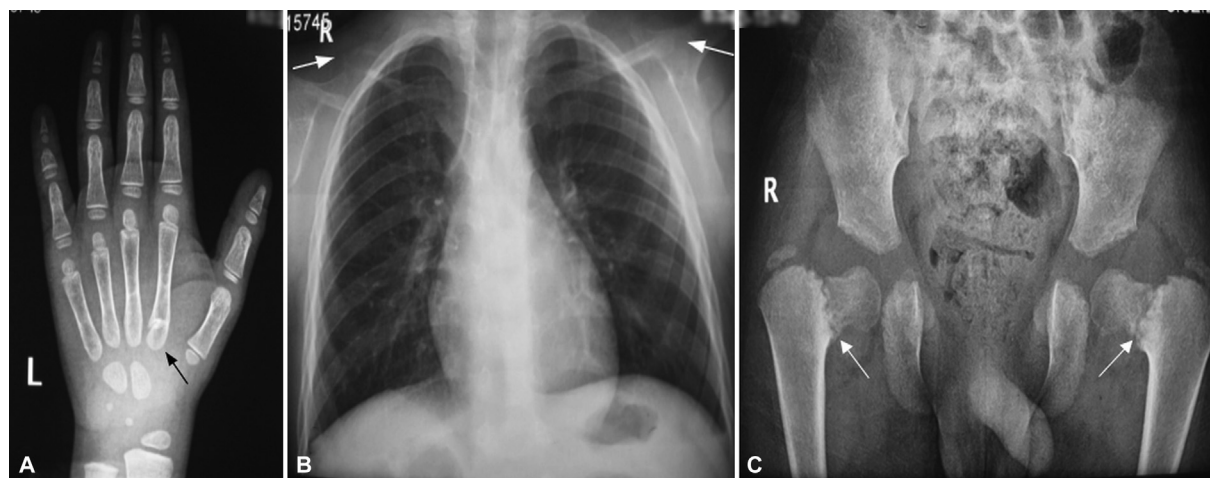


Fig. 25 Cleidocranial dysplasia. Hand radiograph (A) showing an accessory epiphysis at the base of the second metacarpal (black arrow). Chest radiograph (B) demonstrating hypoplastic bilateral lateral clavicles, more pronounced on right (white arrows). Pelvic radiograph (C) showing delayed ossification of pubic bones with resultant pseudo widening and bilateral coxa vara (arrows).

Limitation

Few of the radiographs presented in this review are of suboptimal quality despite maximum efforts from the authors due to the rarity of these disorders and encountering few cases that demonstrate classical findings.

Conclusion

Hand radiographs give important clues to the diagnosis of various skeletal dysplasias; some of these findings are pathognomonic of certain dysplasias. Although it cannot replace a complete skeletal survey in its diagnosis, hand radiographs performed for other indications might alert a radiologist to the diagnosis of an unsuspected skeletal dysplasia.

Funding

None.

Conflict of Interest

None declared.

References

- 1 El-Sobky TA, Shawky RM, Sakr HM, et al. A systematized approach to radiographic assessment of commonly seen genetic bone diseases in children: a pictorial review. *J Musculoskelet Surg Res* 2017;1:25–32
- 2 Handa A, Nishimura G, Zhan MX, Bennett DL, El-Khoury GY. A primer on skeletal dysplasias. *Jpn J Radiol* 2022;40(03):245–261
- 3 Uttarilli A, Shah H, Shukla A, Girisha KM. A review of skeletal dysplasia research in India. *J Postgrad Med* 2018;64(02):98–103
- 4 Orioli IM, Castilla EE, Barbosa-Neto JG. The birth prevalence rates for the skeletal dysplasias. *J Med Genet* 1986;23(04):328–332
- 5 Hall BD. Approach to skeletal dysplasia. *Pediatr Clin North Am* 1992;39(02):279–305
- 6 Mortier GR. The diagnosis of skeletal dysplasias: a multidisciplinary approach. *Eur J Radiol* 2001;40(03):161–167
- 7 Gilsanz V, Ratib O. *Hand Bone Age: A Digital Atlas of Skeletal Maturity*. Berlin: Springer; 2005
- 8 Cavallo F, Mohn A, Chiarelli F, Giannini C. Evaluation of bone age in children: a mini-review. *Front Pediatr* 2021;9:580314
- 9 Skeletal Dysplasia. Slovis TL, Adler BH, Bloom DA, Bulas DI, Coley BD, Donaldson JS. *Caffey's pediatric diagnostic imaging*. Philadelphia, PA: Mosby; 2008
- 10 Faivre L, Cormier-Daire V, Elliott AM, et al. Desbuquois dysplasia, a reevaluation with abnormal and “normal” hands: radiographic manifestations. *Am J Med Genet A* 2004;124A(01):48–53
- 11 OMIM Entry - # 208230 - Progressive Pseudorheumatoid Dysplasia ; PPRD
- 12 Garcia Segarra N, Mittaz L, Campos-Xavier AB, et al. The diagnostic challenge of progressive pseudorheumatoid dysplasia (PPRD): a review of clinical features, radiographic features, and WISP3 mutations in 63 affected individuals. *Am J Med Genet C Semin Med Genet* 2012;160C(03):217–229
- 13 Eash DD, Weaver DD, Brunetti-Pierrri N. Cervical spine stenosis and possible vitamin K deficiency embryopathy in an unusual case of chondrodysplasia punctata and an updated classification system. *Am J Med Genet A* 2003;122A(01):70–75
- 14 Koç U, Karakaş P. Radiological picture of premature baby with manifestation of brachytelephalangic type chondrodysplasia punctata, myelomalacia. *Turk J Pediatr* 2017;59(05):604–609
- 15 Giedion A, Prader A, Fliegel C, Krasikov N, Langer L, Poznanski A. Angel-shaped phalango-epiphyseal dysplasia (ASPED): identification of a new genetic bone marker. *Am J Med Genet* 1993;47(05):765–771
- 16 OMIM entry - # 105835- Angel shaped phalango-epiphyseal dysplasia. (ASPED)
- 17 Mantovani G, Spada A. Mutations in the Gs alpha gene causing hormone resistance. *Best Pract Res Clin Endocrinol Metab* 2006;20(04):501–513
- 18 de Sanctis L, Vai S, Andreo MR, Romagnolo D, Silvestro L, de Sanctis C. Brachydactyly in 14 genetically characterized pseudohypoparathyroidism type Ia patients. *J Clin Endocrinol Metab* 2004;89(04):1650–1655
- 19 Goswami M, Verma M, Singh A, Grewal H, Kumar G. Albright hereditary osteodystrophy: a rare case report. *J Indian Soc Pedod Prev Dent* 2009;27(03):184–188
- 20 Al Kaissi A, Bieganski T, Baranska D, et al. Robinow syndrome: report of two cases and review of the literature. *Australas Radiol* 2007;51(01):83–86

- 21 Patton MA, Afzal AR. Robinow syndrome. *J Med Genet* 2002;39(05):305–310
- 22 Vanhoenacker FM, Van Hul W, Wuyts W, Willems PJ, De Schepper AM. Hereditary multiple exostoses: from genetics to clinical syndrome and complications. *Eur J Radiol* 2001;40(03):208–217
- 23 Kok HK, Fitzgerald L, Campbell N, et al. Multimodality imaging features of hereditary multiple exostoses. *Br J Radiol* 2013;86(1030):20130398
- 24 Jurik AG, Jørgensen PH, Mortensen MM. Whole-body MRI in assessing malignant transformation in multiple hereditary exostoses and enchondromatosis: audit results and literature review. *Skeletal Radiol* 2020;49(01):115–124
- 25 Jurik AG. Multiple hereditary exostoses and enchondromatosis. *Best Pract Res Clin Rheumatol* 2020;34(03):101505
- 26 Palmucci S, Attinà G, Lanza ML, et al. Imaging findings of mucopolysaccharidoses: a pictorial review. *Insights Imaging* 2013;4(04):443–459
- 27 Gholamrezaezhad A, Weinert D, Kosmas C, Young P, Robbin M. Musculoskeletal/Radiological Manifestations of Mucopolidosis II (I-Cell disease) in late adolescence/early adulthood. *Pediatr Endocrinol Diabetes Metab* 2016;22(04):163–169
- 28 Al Kaissi A, Kenis V, Melchenko E, et al. Corrections of lower limb deformities in patients with diastrophic dysplasia. *Orthop Surg* 2014;6(04):274–279
- 29 Girisha KM, Bidchol AM, Graul-Neumann L, et al. Phenotype and genotype in patients with Larsen syndrome: clinical homogeneity and allelic heterogeneity in seven patients. *BMC Med Genet* 2016;17(01):27
- 30 Bicknell LS, Farrington-Rock C, Shafeghati Y, et al. A molecular and clinical study of Larsen syndrome caused by mutations in FLNB. *J Med Genet* 2007;44(02):89–98
- 31 Cirillo RL Jr. Pediatric case of the day. Rubinstein-Taybi syndrome. *Radiographics* 1997;17(06):1604–1605
- 32 Kumar S, Suthar R, Panigrahi I, Marwaha RK. Rubinstein-Taybi syndrome: Clinical profile of 11 patients and review of literature. *Indian J Hum Genet* 2012;18(02):161–166
- 33 Panda A, Gamanagatti S, Jana M, Gupta AK. Skeletal dysplasias: A radiographic approach and review of common non-lethal skeletal dysplasias. *World J Radiol* 2014;6(10):808–825
- 34 Renaud A, Aucourt J, Weill J, et al. Radiographic features of osteogenesis imperfecta. *Insights Imaging* 2013;4(04):417–429
- 35 Oz B, Olmez N, Memis A. Osteogenesis imperfecta: a case with hand deformities. *Clin Rheumatol* 2005;24(05):565–568
- 36 Stark Z, Savarirayan R. Osteopetrosis. *Orphanet J Rare Dis* 2009;4(01):5
- 37 Ihde LL, Forrester DM, Gottsegen CJ, et al. Sclerosing bone dysplasias: review and differentiation from other causes of osteosclerosis. *Radiographics* 2011;31(07):1865–1882
- 38 Olusola-Bello M, Olatunji A, Toyobo O. Hajdu-Cheney syndrome: a rare acro-osteolytic disorder. *West Afr J Radiol* 2018;25(02):124
- 39 Palav S, Vernekar J, Pereira S, Desai A. Hajdu-Cheney syndrome: a case report with review of literature. *J Radiol Case Rep* 2014;8(09):1–8
- 40 Kozłowski K, Campbell JB, Azouz ME, Sprague P. Metaphyseal chondrodysplasia, type Jansen. *Australas Radiol* 1999;43(04):544–547
- 41 Sutton VR, Hyland JC, Phillips WA, Schlesinger AE, Brill PW. A dominantly inherited spondylometaphyseal dysplasia with “corner fractures” and congenital scoliosis. *Am J Med Genet A* 2005;133A(02):209–212
- 42 Muensterer OJ, Berdon W, McManus C, et al. Ellis-van Creveld syndrome: its history. *Pediatr Radiol* 2013;43(08):1030–1036
- 43 Faivre L, Le Merrer M, Baumann C, et al. Acromicric dysplasia: long term outcome and evidence of autosomal dominant inheritance. *J Med Genet* 2001;38(11):745–749
- 44 Langer LO, Garrett RT. Acromesomelic dysplasia. *Radiology* 1980;137(02):349–355